

Testing and Modeling Two Rockfill Materials

A. Varadarajan¹; K. G. Sharma²; K. Venkatachalam³; and A. K. Gupta⁴

Abstract: Modeled rockfill materials consisting of rounded and angular particles obtained from two dam sites are subjected to drained triaxial tests using large size specimens. An elastoplastic constitutive model based on the disturbed state concept is adopted to characterize the behavior of the modeled rockfill materials. The material parameters for the two rockfill materials are determined from the experimental results. The variation of the material parameters with respect to the size of the particles for the rockfill material with the rounded particle is, in general, opposite to that for the rockfill material with the angular particles. The model is shown to provide satisfactory prediction of the behavior of the rockfill materials tested. Material parameters are predicted for prototype size of rockfill materials.

DOI: 10.1061/(ASCE)1090-0241(2003)129:3(206)

CE Database keywords: Rockfill structures; Models; Triaxial tests.

Introduction

Rockfill dams are increasingly used because of their inherent flexibility, capacity to absorb large seismic energy, and adaptability to various foundation conditions. The use of modern earth and rock moving equipment and locally available materials make such dams economical as well. Rockfill materials consist primarily of angular to subangular particles obtained by blasting parent rock or rounded/sub-surrounded particles collected from river beds. The behavior of the rockfill materials is affected by such factors as mineralogical composition, particle grading, size and shape of particles, and stress conditions. Testing and modeling of the behavior of the rockfill materials are essential prerequisites to the realistic analysis and design of rockfill dams. This paper deals with laboratory testing and constitutive modeling of rockfill materials collected from two dam sites.

Review

Rockfill materials contain particles of large size, and testing of such rockfill materials would require equipment of formidable dimensions. Therefore, the size of the rockfill materials for testing are reduced using modeling techniques. The various modeling techniques used, testing of the rockfill materials, and the model-

ing of behavior of the rockfill materials are briefly reviewed herein.

Four modeling techniques are used to reduce the size of the rockfill materials, viz. the scalping technique (Zeller and Wullemann 1957), parallel gradation technique (Lowe 1964), generation of quadratic grain-size distribution curve (Fumagalli 1969), and replacement technique (Frost 1973). Of these, the parallel gradation method was considered most appropriate (Ramamurthy and Gupta 1986).

Large scale triaxial testing equipment has been used to conduct tests on rock fragments and rockfill materials. Specimen diameter in these tests ranged from 15.2 to 500 mm, the maximum size of particles ranged from 3.8 to 100 mm, and the maximum confining pressure ranged from 0.69 to 13.8 MPa (Hall and Gordon 1963; Marsal 1967; Fumagalli 1969; Marachi et al. 1972; Thiers and Donovan 1981; Ansari and Chandra 1986; Venkatachalam 1993). These researchers conducted tests on a wide range of rockfill materials. They have concluded that (1) the stress-strain behavior of the rockfill materials is nonlinear, inelastic and stress dependent, (2) an increase in confining pressure tends to increase the value of peak deviator stress, axial strain, and volumetric strain at failure, and (3) an increase in the size of the particles results in an increase in volumetric strain at the same confining pressure. They found that the behavior of the rockfill depends on mineral composition, grain size, shape, gradation, and relative density of the rockfill.

The constitutive models used to characterize the behavior of the rockfill materials are mostly based on linear elastic and nonlinear elastic theories. Hyperbolic models are often adopted to depict the behavior of rockfill materials, for example, Kulhawy and Duncan (1972); Venkatachalam (1993); Saboya and Bryne (1993).

Scope

The scope of the investigation was to conduct triaxial tests on modeled rockfill materials, to develop a constitutive model using an elastoplastic theory to predict their stress-strain-volume change behavior and to propose a procedure to predict material parameters for prototype rockfill materials.

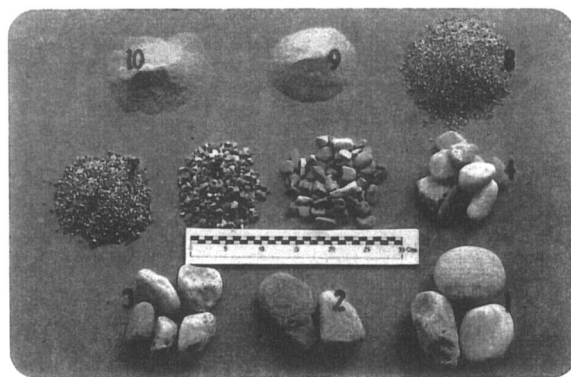
¹Dogra Chair Professor, Dept. of Civil Engineering, Indian Institute of Technology, Delhi, Hauz Khas, New Delhi 110 016, India. E-mail: avrajan@civil.iitd.ernet.in

²Professor, Dept. of Civil Engineering, Indian Institute of Technology, Delhi, Hauz Khas, New Delhi 110 016, India.

³Director, CSMRS, Hauz Khas, New Delhi 110 016, India.

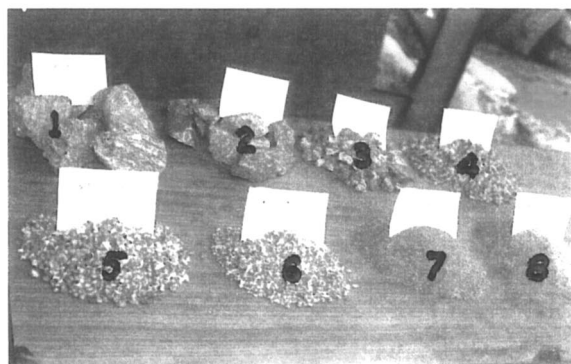
⁴Assistant Professor, Department of Civil Engineering, R.E.C., Hamirpur.

Note. Discussion open until September 1, 2003. Separate discussions must be submitted for individual papers. To extend the closing date by one month, a written request must be filed with the ASCE Managing Editor. The manuscript for this paper was submitted for review and possible publication on December 8, 2000; approved on June 25, 2002. This paper is part of the *Journal of Geotechnical and Geoenvironmental Engineering*, Vol. 129, No. 3, March 1, 2003. ©ASCE, ISSN 1090-0241/2003/3-206-218/\$18.00.



No.	1	2	3	4	5
Particle Size (mm)	80-60	60-50	50-40	40-25	25-10
No.	6	7	8	9	10
Particle Size (mm)	10-4.75	4.75-2.0	2.0-0.425	0.425-0.075	<0.075

(a)



No.	1	2	3	4
Particle Size (mm)	80-50	50-25	25-12.5	12.5-6.3
No.	5	6	7	8
Particle Size (mm)	6.3-4.75	4.75-2.0	2.0-0.425	0.425-0.075

(b)

Fig. 1. (a) Ranjit Sagar dam material (Scale is 30 cm long) and (b) Purulia dam material

Laboratory Tests

Rockfill Materials

For the present study, rockfill materials were obtained from the Ranjit Sagar Hydropower Project located in the Gurdaspur district of the Punjab state in North India and the Purulia Pumped Storage Hydroelectric Project located in the Purulia district of the West Bengal State in the eastern part of India. The rockfill material used in the Ranjit Sagar Project is an alluvial material consisting of rounded/subrounded particles up to 320 mm in size [Fig. 1(a)]. The material is derived from Upper Shivalik rock of sedimentary origin. The rockfill material used in the Purulia Project was obtained by blasting rock and consists of angular to subangular particles up to 1,200 mm in size [Fig. 1(b)]. The rock is of metamorphic origin. The lithology/mineralogy of the materials is given in Table 1.

Modeled Rockfill Materials

Representative rockfill materials were collected from the two project sites. The particles of the two materials were subjected to impact, crushing and Los Angeles abrasion tests as per Indian Standard Code IS-2386 (Part IV) (1963). From these tests, aggregate impact value, aggregate crushing value, and Los Angeles abrasion value were determined for the two materials and are presented in Table 1. These values show that rockfill particles from the Ranjit Sagar site were stronger than those from the Purulia site. The gradation curves of these materials are shown in Figs. 2 and 3. From the materials, three modeled gradation curves were derived using the parallel gradation modeling technique (Lowe 1964) with maximum particle sizes of 80, 50, and 25 mm, respectively, as shown in Figs. 2 and 3. Values of the maximum and minimum dry densities for the modeled materials were determined and are presented in Table 1.

Experimental Program

Consolidated drained triaxial tests were conducted on the modeled rockfill materials. For testing, a dry density corresponding to 87% of relative density was adopted (Table 1). The range of confining pressures was chosen keeping in view the stress levels in the proposed dams. Details of the tests are given in Table 2.

To test the rockfill materials, the large size triaxial testing facility at the Central Soil and Materials Research Station, New Delhi, India, a premier Government of India Research Station which provides laboratory and field testing services for various river valley projects was used. Two specimen sizes, 381 mm diameter by 813 mm long, and 500 mm diameter by 600 mm long were used for testing. Details of the two triaxial cells used for the two sizes of specimen are shown in Figs. 4 and 5. Details of equipments used are given in Table 2.

Experimental Procedure

The quantity of various sizes of rockfill materials required to achieve the gradation of the modeled rockfill material for preparing the specimen at the specified density was determined by weight. The individual fractions were mixed thoroughly after wetting the material to 3 to 4% moisture content. The sample was prepared using a split mold. The mix was divided into six equal parts for compacting into six layers inside the split mold. Each layer of the fill was compacted using a vibrator with a frequency of 60 cycles/s. The procedure was evolved after several trials to get the required density. The sample was saturated by allowing water to pass through the base of the triaxial cell, and using a top drainage system for removing air voids. The sample was first subjected to the required consolidation pressure and was then sheared by applying axial loading so as to achieve a rate of loading of 1 mm/min. Readings of vertical displacement, volume change, and axial loads were taken at periodic intervals. A few tests were repeated to verify reproducibility of the results. The results obtained from the two triaxial cells were compared and were found to be nearly same. Complete details of testing are given by Gupta (2000).

Experimental Results

The stress-strain-volume change behavior of the three sizes of modeled rockfill materials for the Ranjit Sagar Dam site and the Purulia Dam site are shown in Figs. 6 and 7, respectively. Both

Table 1. Rockfill Material Characteristics

Characteristics	Ranjit Sagar			Purulia		
Rockfill source	Alluvium			Blasting		
Lithology/mineralogy	Sedimentary materials including conglomerate, sandstone, quartzite, shale, claystone, grits of chart and jasper, other materials of older rocks, and recent alluvium			Metamorphic rock with minerals including quartz, biotite and feldspar with other accessory minerals like tourmaline and hornblende		
Particle shape	Rounded/subrounded			Angular/subangular		
Aggregate impact value ^a	28.70%			36.2%		
Aggregate crushing value ^a	36.50%			39.5%		
Los Angeles abrasion value ^a	23.8%			48.8%		
D_{\max} (mm)	25	50	80	25	50	80
D_{50} (mm)	3.8	7.6	12.0	5.0	9.6	15.8
Unit weight (dry)						
γ_{\max} (kN/m ³)	22.0	22.0	22.9	21.6	21.6	21.7
γ_{\min} (kN/m ³)	19.2	19.1	19.5	17.0	17.2	17.4
γ (kN/m ³) corresponding to 87% of relative density	21.6	21.6	22.4	20.9	20.9	21.0

^aDetermined as per Indian Standard Code IS: 2386 (Part IV) 1963.

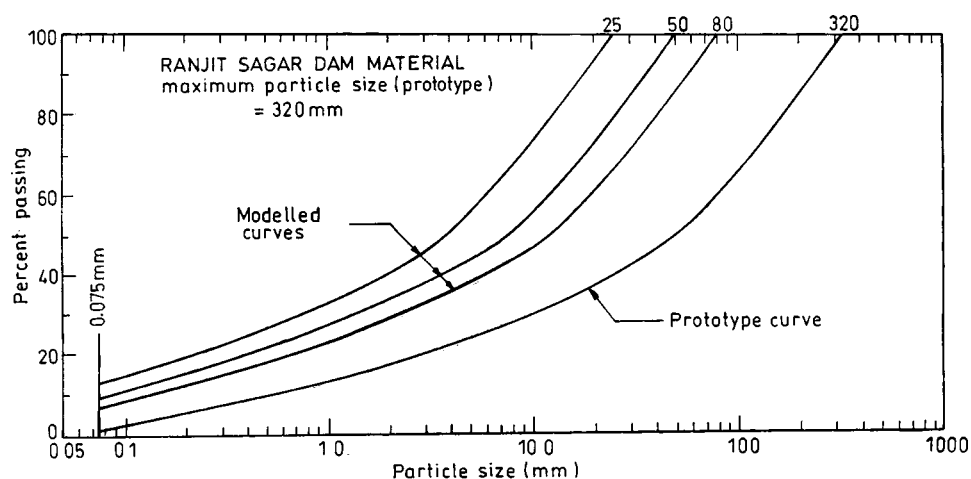
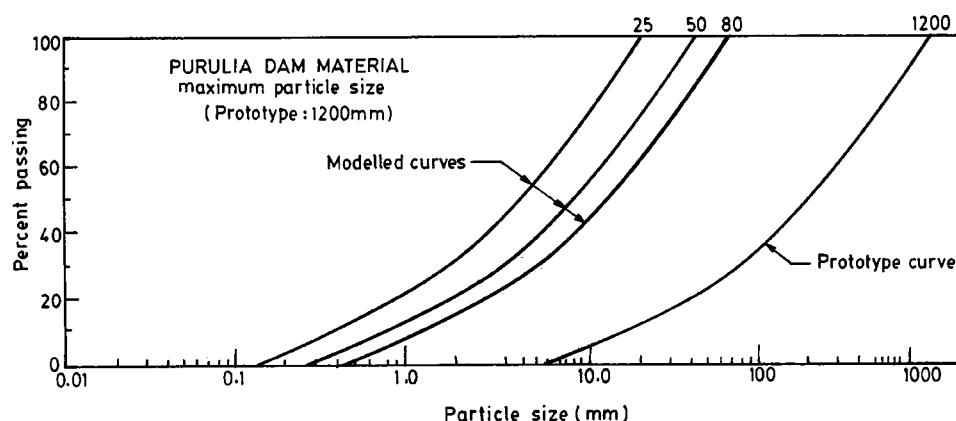
**Fig. 2.** Grain-size distribution for prototype and modelled rockfill material from Ranjit Sagar dam site**Fig. 3.** Grain-size distribution for prototype and modelled rockfill material from Purulia dam site

Table 2. Details of Drained Triaxial Tests Conducted

S.No.	Details	Name of Project	
		Ranjit Sagar Dam	Purulia Dam
1	Maximum particle size, D_{max} (mm)	25,50,80	25,50,80
2	Average particle size, D_{50} (mm)	3.8,7.6,12.0	5.0,9.6,15.8
3	Confining pressure, σ_3 (kPa)	350,700,1100,1400	300,600,900,1200
4	Triaxial cell (1), Specimen size: length=813 mm, diameter=381 mm Confining pressure applied by an air-water pressure system: maximum confining pressure=3 MPa, Axial load applied by hydraulic pressure unit: maximum axial load=875.7 kN		
5	Triaxial Cell (2), Specimen size: length=600 mm, diameter=500 mm Confining pressure applied by an air-water pressure system: maximum confining pressure=3 MPa, Axial load applied by an actuator system: maximum axial load=2258 kN		
6	Axial strain measurement: Dial gauge/LVDT		
7	Volumetric strain measurement: Burette/Transducer		

materials showed an increase in axial strain and volumetric strain at failure with increasing confining pressure and particle size. The values of axial strain at failure for the Ranjit Sagar rockfill material were higher than those for the Purulia rockfill material. A continuous increase in compressive volumetric strain was observed throughout the axial loading for the rockfill material from the Ranjit Sagar dam site, but the material from the Purulia dam

site showed an increase in compressive volumetric strain during initial loading and a decrease in compressive volumetric strain on subsequent loading.

It is interesting to note that the volume change behaviors of the two rockfill materials are significantly different from each other. During the shearing stage of the triaxial test, compression, rear-

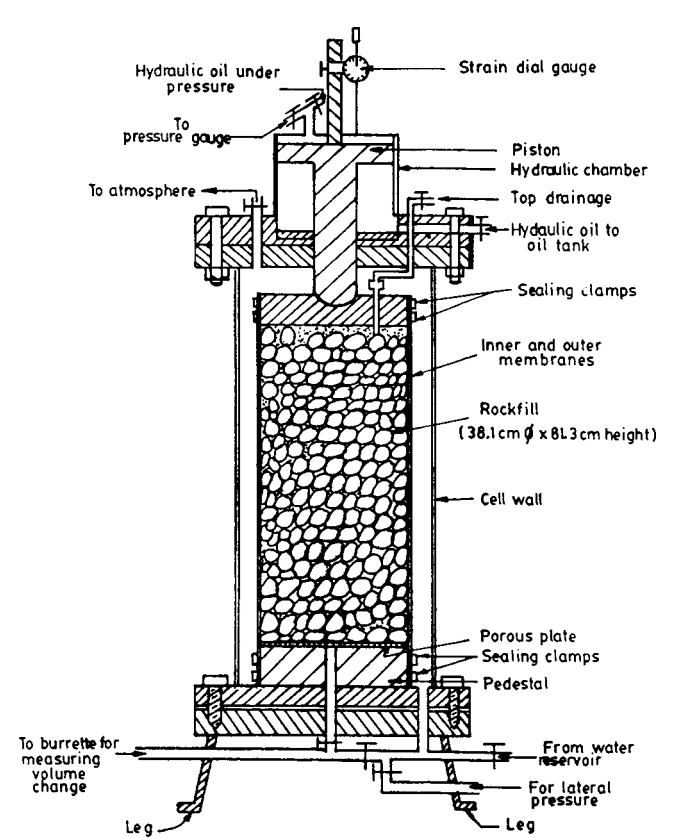


Fig. 4. Triaxial cell for 381 mm diameter and 813 mm high specimen

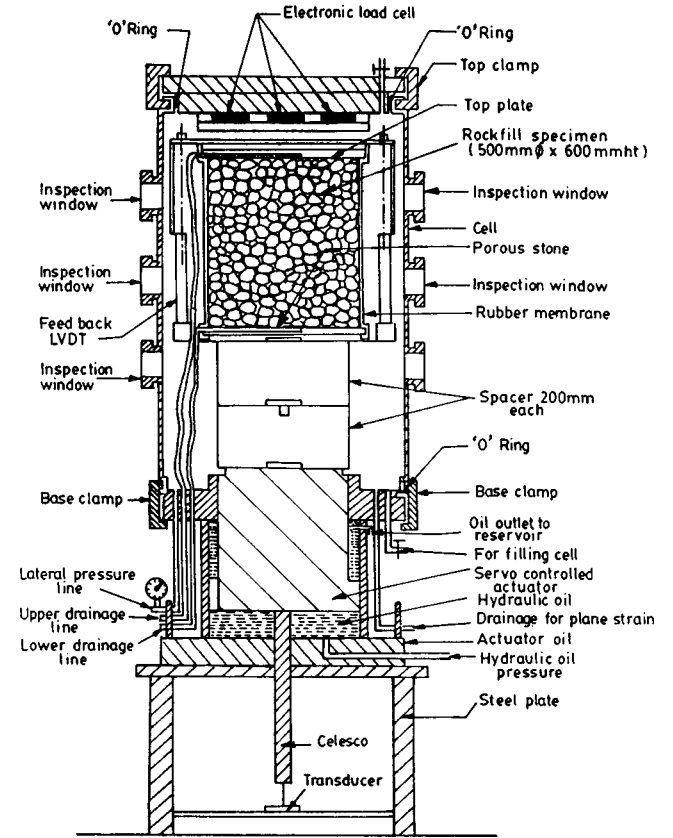
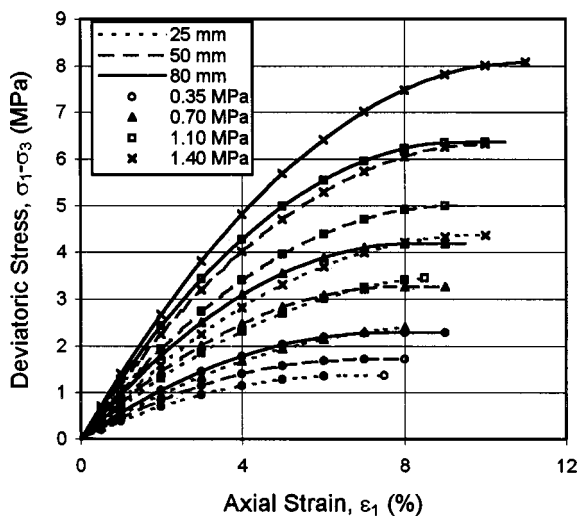
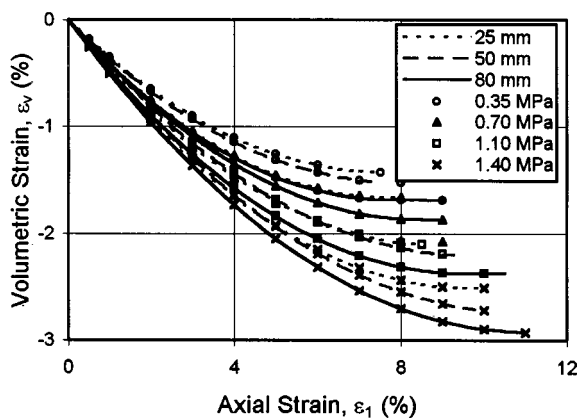


Fig. 5. Triaxial cell for 500 mm diameter and 600 mm high specimen



(a) Stress-Strain Behavior

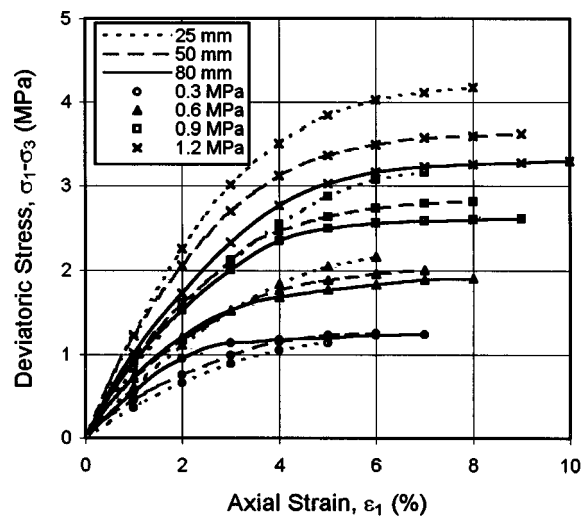


(b) Volume Change Behavior

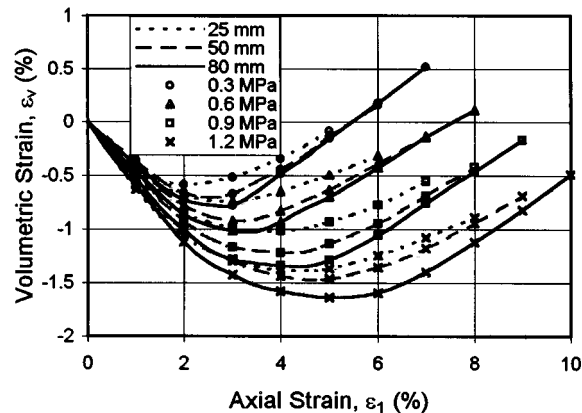
Fig. 6. Stress-strain-volume change relationship for rockfill material from Ranjit Sagar Dam site, $D_{\max}=25, 50,$ and 80 mm

rangement, and breakage of particles take place. The Ranjit Sagar rockfill material undergoes volume compression due to compression of the particles and rearrangement of the particles due to the sliding of the rounded particles. The breakage of the particles also adds to the volume compression. Therefore, this rockfill material exhibits continuous volume compression throughout the test. In the Purulia rockfill material, volume compression takes place due to compression and breakage of the particles. The angular particles provide a high degree of interlocking and cause dilation during shearing. During the initial phase of shearing, dilatancy is less and therefore net volume compression takes place. During the latter phase of shearing, dilatancy is more, leading to volume expansion.

Particle breakage was observed during shearing. The breakage is expressed quantitatively by the breakage factor B_g . The value of B_g is calculated from the sieve analysis of rockfill sample as follows. Before testing, the sample is sieved using a set of standard sieves (80 to 0.075 mm in size) and the percentage of particles retained in each sieve is calculated. After testing, the sample is again sieved and the percentage of particles retained is calculated. Due to the breakage of particles, the percentage of particles retained in large size sieves will decrease and the percentage of particles retained in small size sieves will increase. The sum of decreases in the percentage retained will be equal to the sum of



(a) Stress-Strain Behavior



(b) Volume Change Behavior

Fig. 7. Stress-strain-volume change relationship for rockfill material from Purulia Dam site, $D_{\max}=25, 50,$ and 80 mm

increases in the percentage retained. The sum of decreases (or increases) is the value of the breakage factor B_g (Marsal 1967). The breakage factor is affected by the particle size and the confining pressure (Fig. 8). It is noted that the breakage factor increases with the size of the particles and the confining pressure. It is also noted that the effects of the size of particles and the confining pressure are more pronounced for the Purulia material than for the Ranjit Sagar material. The high value of the breakage factor in the Purulia material is due to the relatively low strength of the particles. (Table 1). Furthermore, the angular particles are more susceptible to breakage than the rounded particles. The values of the maximum principal stress ratio $(\sigma_1/\sigma_3)_{\max}$ and B_g obtained for these materials have been shown in Fig. 9 along with the results of Marachi et al. (1969) and Venkatachalam (1993). The results of the two rockfill materials lie within the two limits shown in the figure.

The angle of shearing resistance (ϕ) for the two rockfill materials is shown in Table 3. The angle of shearing resistance increases with the size of the particles for the Ranjit Sagar material, but the opposite trend is observed for the Purulia material. It is significant to note that the two rockfill materials show opposite trends with respect to variation of the angle of shearing resistance with the size of the particles. As the average particle size increases in a granular material, lower-initial void ratio, which pro-

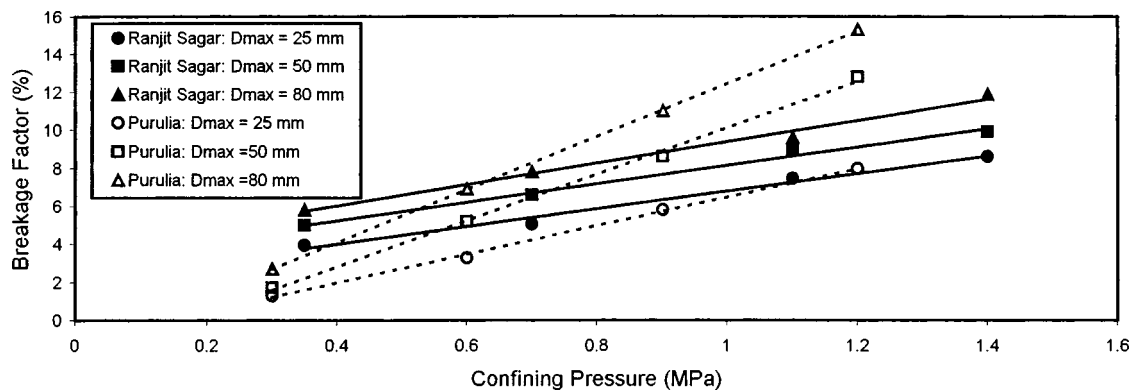


Fig. 8. Variation of breakage factor with confining pressure

vides greater interlocking, is achieved for the same compactive effort (Lambe and Whitman 1969). But a greater degree of breakage of particles also occurs with the larger particles because of the greater force per contact (Lambe and Whitman 1969). The effect of the increase in interlocking is to increase the shearing resistance, while the effect of breakage of the particles is to decrease the shearing resistance. In the case of the Ranjit Sagar rockfill material, the rate of increase in the breakage factor with increase in particle size is low (an increase of 3.25% in the breakage factor at a confining pressure of 1.4 MPa). Therefore, the net effect is an increase in the angle of shearing resistance with particle size. In the case of the Purulia rockfill material, the rate of increase in the breakage factor with particle size is high (an increase of 7.3% in the breakage factor at the confining pressure of 1.2 MPa). As such, the net effect is a decrease in the angle of shearing resistance with particle size. In general (Table 3) the alluvial materials (Ranjit Sagar) showed an increase in the angle of shearing resistance with an increase in the size of the particles (for example, Sudhindra et al. 1991; Venkatachalam 1993) and the materials produced by rock blasting (Purulia) showed a decrease in the

angle of the shearing resistance with an increase in the size of the particles (Table 3, Marachi et al. 1972).

Constitutive Model

The disturbed state concept (DSC) developed by Desai (1994, 2001) has been adopted to characterize the behavior of the rockfill materials. The constitutive model based on the DSC allows for a number of factors such as irreversible plastic strains, plastic hardening, nonassociative (frictional) aspects, and degradation due to breakage of particles that were observed in the rockfill materials. This model is believed by the authors to be better suited to the case at hand than the available linear and nonlinear elastic models used for rockfill materials. The DSC is briefly explained as follows. As the material deforms under applied loading, an initially intact material undergoes microstructural changes which may involve reorientation of particles, damage, microcracking, breakage of particles, and induced anisotropy. During such microstructural changes, the material may remain continuous or may become discontinuous. The latter implies the traditional damage model (Muhlhaus and Vardoulakis 1987; van Mier 1991). In the limit, the entire material approaches the fully adjusted state. In the DSC, the observed response is defined with respect to the responses of two reference states of the material, called the relative intact state and fully adjusted state. A disturbance function, D is defined to express the observed response in terms of the responses under the relative intact and fully adjusted states.

There are similarities between the well-known damage concept (Kachanov 1958, 1986; Lemeire 1984, 1985) and the DSC, e.g., in the form of the disturbance function D described subsequently. This form is representative of many natural systems that exhibit modification in their states, e.g., decay and degradation. It is considered that damage is a special case of the DSC. The term *disturbance* is used in the DSC, as it provides a more appropriate terminology in the sense that many materials may deform without experiencing microcracking and fracturing and without losing continuity.

Complete details of the DSC are given in various publications Desai (1995, 2001). The salient features of the DSC as applied to rockfill materials are described herein. In the DSC, the material response is expressed in terms of the responses in the continuous (relative intact, RI) and the discontinuous (fully adjusted, FA) parts as

$$\sigma_{ij}^a = (1 - D)\sigma_{ij}^i + D\sigma_{ij}^c \quad (1)$$

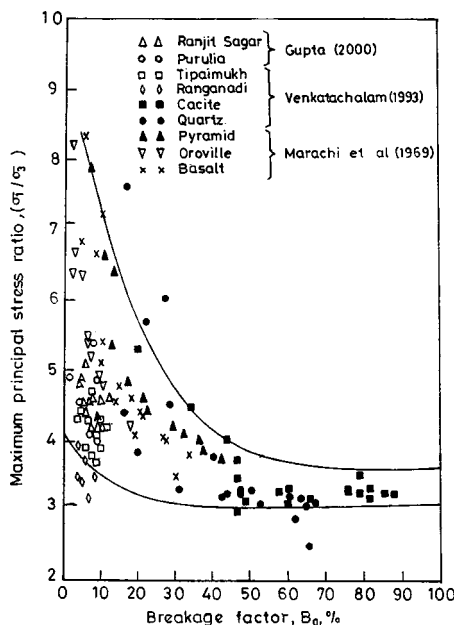


Fig. 9. Relationship between principal stress ratio and breakage factor

Table 3. Material Parameters for Rockfill Materials

Material constants	Ranjit Sagar Dam Material D_{\max} (mm)				Purulia Dam Material D_{\max} (mm)			
	25	50	80	320	25	50	80	1200
Elasticity								
k	193.69	220.34	253.63	343.35	167.07	286.02	451.13	4390.4
n'	0.6386	0.6683	0.7146	0.8141	0.8162	0.6991	0.4068	0.0866
μ	0.31	0.30	0.29	0.30	0.34	0.33	0.31	0.33
Ultimate								
γ	0.0780	0.0840	0.0912	0.1083	0.0760	0.0680	0.0600	0.0353
β	0.730	0.732	0.743	0.730	0.730	0.720	0.720	0.720
Phase change, n	3	3	3	3	3	3	3	3
Hardening								
a_1	$0.65E-4$	$0.30E-4$	$0.985E-5$	$1.E-6$	$0.32E-4$	$0.4E-4$	$0.5E-4$	$1.E-4$
η_1	0.4675	0.5600	0.7618	1.2865	0.7000	0.6800	0.6900	0.5527
Non-associative, κ	0.23	0.23	0.22	0.23	0.22	0.22	0.20	0.22
Disturbance								
A	0.016	0.032	0.050	0.196	0.0414	0.03	0.02	0.0041
B	6.0	7.34	8.84	13.80	10.993	9.00	7.2	2.7861
ϕ degrees	31.5	33.2	35.4	40.31	32.5	31.4	30.6	26.62

where the superscripts a , i , and c denote observed (averaged), RI, and FA states, respectively. Based on the analysis of the experimental data in this study the coupling (disturbance) function between the two states is expressed as

$$D = \frac{\xi_D}{A + B\xi_D} \quad (2)$$

where A and B =disturbance parameters and ξ_D =deviatoric part of the plastic strain increment (dE_{ij}^p) trajectory given by

$$\xi_D = \int (dE_{ij}^p dE_{ij}^p)^{1/2} \quad (3)$$

The relative intact state is modeled as a nonassociated elasto-plastic hardening response and is characterized by the hierarchical single surface (HISS) δ_1 model, (Desai et al. 1986; Desai and Wathugala 1987; Varadarajan et al. 1999; Desai 2001) with a yield function as

$$F = \frac{J_{2D}}{P_a^2} - \left[-\alpha \left(\frac{J_1}{P_a} \right)^n + \gamma \left(\frac{J_1}{P_a} \right)^2 \right] (1 - \beta S_r)^m = 0 \quad (4)$$

where J_{2D} =second invariant of the deviatoric stress tensor; J_1 =first invariant of the stress tensor; P_a =atmospheric pressure; γ and β =material response functions associated with the ultimate behavior; $m = -0.5$; α =hardening function; n =phase change parameter; and S_r =stress ratio given by

$$S_r = \frac{\sqrt{27} J_{3D}}{2 J_{2D}^{1.5}} \quad (5)$$

in which J_{3D} =third invariant of the deviatoric stress tensor.

For the nonassociative δ_1 model, the plastic potential function Q is defined as a modification of F with α replaced by α_Q i.e.

$$Q = \frac{J_{2D}}{P_a^2} - \left[-\alpha_Q \left(\frac{J_1}{P_a} \right)^n + \gamma \left(\frac{J_1}{P_a} \right)^2 \right] (1 - \beta S_r)^m \quad (6)$$

where

$$\alpha_Q = \alpha + \kappa(\alpha_0 - \alpha)(1 - r_v) \quad (7)$$

in which κ =nonassociative parameter; α_0 =value of α at the beginning of shear loading; and

$$r_v = \frac{\xi_v}{\xi} \quad (8)$$

$$\xi_v = \int \frac{|d\varepsilon_v^p|}{\sqrt{3}} \quad (9)$$

where ξ_v =volumetric part of the total plastic strain trajectory.

The HISS yield function can also be expressed as

$$F = \frac{J_{2D}}{P_a^2} - F_b F_s = 0 \quad (10)$$

where F_b and F_s are the basic and shape functions, respectively.

As a simplification, it is assumed that strains in the RI and FA states are equal that is, there is no motion between the RI and FA states. An additional assumption is made that the material carry hydrostatic stresses which are the same in the RI and FA states, that is $J_1^c = J_1^i$ (Desai 2001).

Material Parameters

The procedure for the determination of material parameters required in the model has been described in detail in various references (for example, Varadarajan and Desai 1993; Desai 2001). The procedure is briefly presented herein.

One of the steps in the determination of material parameters using DSC is to estimate the stress-strain response of the rockfill materials at the RI state. In the present study, the following procedure is adopted. On the basis of the plot presented by Marachi et al. (1972) between B_g and (σ_1/σ_3) at failure, the observed values of (σ_1/σ_3) for the rockfill material at failure are expressed as

$$\left(\frac{\sigma_1}{\sigma_3}\right) = \frac{1+B_g}{A_d B_g + B_d} \quad (11)$$

where A_d and B_d =constants. These constants are determined using the values of (σ_1/σ_3) at failure and the values of B_g at various confining pressures for each size of the rockfill material. It is assumed at the RI state that there will not be any breakage of particles and therefore, the value of B_g will be zero. Thus, at the RI state, the value of (σ_1/σ_3) at failure is determined with $B_g = 0$ in Eq. (11) as

$$\left(\frac{\sigma_1}{\sigma_3}\right) = \frac{1}{B_d} \quad (12)$$

A hyperbolic relationship is then used to depict the stress-strain response of the rockfill material at the RI state as

$$(\sigma_1 - \sigma_3) = \frac{\varepsilon_1}{a + b\varepsilon_1} \quad (13)$$

where $(\sigma_1 - \sigma_3)$ =deviator stress, and ε_1 =axial strain. The value of b is assumed to be equal to the stresses corresponding to the value of B_d and $a = 1/E_i$ where E_i is the initial tangent modulus. The value of E_i for the RI state is taken to be the same as for the observed state, since the difference in behavior between the two states at the initial stages of loading is expected to be insignificant.

Disturbance Parameters

Rearranging Eq. (1) and based on the fact that σ_{ij}^a and σ_{ij}^i lie on the same deviatoric plane, perpendicular to the hydrostatic axis, such that $J_1^c = J_1^i$, yields

$$\sqrt{J_{2D}^a} = \sqrt{J_{2D}^i}(1-D) \quad (14)$$

where a and i superscripts denote the observed (averaged) and RI states, respectively.

Eq. (14) can be rearranged as

$$D = 1 - \frac{\sqrt{J_{2D}^a}}{\sqrt{J_{2D}^i}} \quad (15)$$

The values of D are found from Eq. (15) at each of the observed points of the stress-strain curve for every test. The values used in the determination of the various DSC parameters are based on the trajectory of plastic strain ξ , expressed as

$$\xi = \int (d\varepsilon_1^p \times d\varepsilon_1^p + d\varepsilon_2^p \times d\varepsilon_2^p + d\varepsilon_3^p \times d\varepsilon_3^p)^{1/2} \quad (16)$$

The values of ξ , ξ_v , and ξ_D (volumetric and deviatoric parts of ξ , respectively) are obtained at the j th point of the observed stress-strain curve as

$$\xi = \sum_{i=1}^j d\xi = \sum_{i=1}^j (d\varepsilon_1^p{}^2 + d\varepsilon_2^p{}^2 + d\varepsilon_3^p{}^2)^{1/2} \quad (17)$$

$$\xi_v = \sum_{i=1}^j d\xi_v = \sum_{i=1}^j \frac{|d\varepsilon_1^p + d\varepsilon_2^p + d\varepsilon_3^p|}{\sqrt{3}} \quad (18)$$

$$\xi_D = \sum_{i=1}^j d\xi_D = \sum_{i=1}^j (d\xi^2 - d\xi_v^2)^{1/2} \quad (19)$$

The values of ξ_D are also determined at each of the observed points of the stress-strain curve for every test. Using the values of D and ξ_D in Eq. (2), the disturbance parameters A and B are determined for each test. The average of the values of the distur-

bance parameters for all the tests is taken as the overall disturbance parameter for a particular size of the rockfill material.

Ultimate Parameters

After the disturbance parameters are known, the value of D is known at all the observed points and Eq. (1) can be rearranged to yield

$$\sigma_{ij}^i = \frac{\sigma_{ij}^a}{1-D} - \frac{D}{1-D} \left(\frac{J_1^i}{3} \right) \delta_{ij} \quad (20)$$

Thus, the stress at the RI state, σ_{ij}^i can be computed from Eq. (20) for the observed (averaged) stress, σ_{ij}^a values. At the ultimate stage, the value of α approaches zero; thus for the RI state, the HISS- δ_1 yield surface degenerates to an open surface intersecting the J_1^i axis at infinity. Using this condition in the yield function, i.e., Eq. (4), the slope of the ultimate line is derived as

$$\frac{J_1^i}{\sqrt{J_{2D}^i}} = \left[\frac{(1 - \beta S_r)^{1/2}}{\gamma} \right]^{1/2} \quad (21)$$

where $S_r = 1$ for compression and $S_r = -1$ for extension tests. The ultimate parameters are found by conducting a least-squares analysis on Eq. (21). For this, the values of J_1 and $\sqrt{J_{2D}}$ corresponding to the ultimate stresses of at least two triaxial tests are required. The ultimate parameters γ and β can also be found from the angle of internal friction in the compression side, ϕ_c and the angle of internal friction in the extension side, ϕ_E as follows, (Desai 2001).

$$\beta = \frac{1 - p'}{1 + p'} \quad (22)$$

where

$$p' = \left(\frac{p_1}{p_2} \right)^{-4} \quad (23)$$

in which

$$p_1 = [\sqrt{\gamma}(1 - \beta)^{-1/4}]_c = \frac{2}{3} \left(\frac{\sin \phi_c}{3 - \sin \phi_c} \right) \quad (24)$$

$$p_2 = [\sqrt{\gamma}(1 + \beta)^{-1/4}]_E = \frac{2}{3} \left(\frac{\sin \phi_E}{3 + \sin \phi_E} \right) \quad (25)$$

After finding the value of β from Eq. (22), the value of γ is found from Eqs. (24) or (25).

In the present analysis, in the absence of observed results from other stress paths, the friction angles in the compression and extension sides of the yield surface are assumed to be the same, i.e., $\phi_C = \phi_E$.

Phase Change Parameter

The phase change parameter n is calculated using the zero plastic volume change condition $\partial F / \partial J_1 = 0$. Based on Eq. (4), this leads to the expression for n as

$$n = \frac{2}{1 - \left(\frac{J_{2D}}{J_1^2} \right) \frac{1}{F_s \gamma}} \quad \text{at zero volume change} \quad (26)$$

The value of n is calculated using this equation for each test. An average of n values for different tests is taken as an overall value for n for the material.

Table 4. Details of Tests used for Group A and Group B Predictions

Size of particle (mm)	Ranjit Sagar Material σ_c Value (MPa)			Purulia Material σ_c Value (MPa)		
	Group A	Group B	Figure number	Group A	Group B	Figure number
25	0.35	1.1	10,11	0.30	—	14
50	0.70	—	12	—	0.60	15
80	1.40	—	13	1.2	0.60	16,17

Hardening Parameters

The hardening function α is assumed to be a function of a single parameter ξ as

$$\alpha = \frac{a_1}{\xi^{\eta_1}} \tag{27}$$

where a_1 and η_1 = material parameters and ξ = trajectory of plastic strain as

$$\xi = \int (d\varepsilon_{ij}^p d\varepsilon_{ij}^p)^{1/2} \tag{28}$$

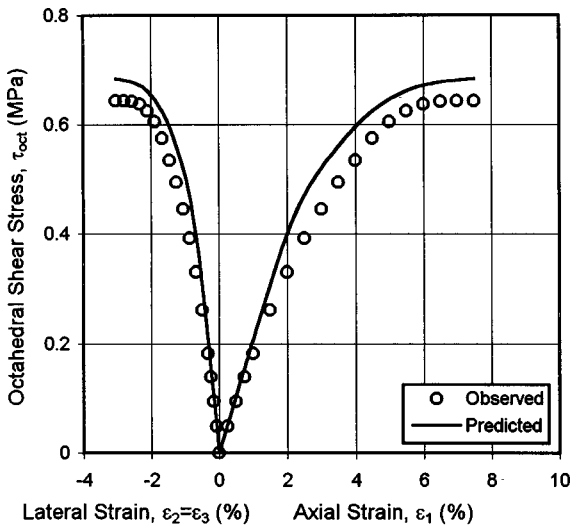
For each test, at all the observed points of the stress-strain curve, the value of ξ is known. The value of the hardening function for the observed points was calculated using the yield func-

tion, i.e., Eq. (4). Substituting the values for α and ξ in Eq. (27) and conducting a least-squares analysis, the hardening parameters a_1 and η_1 were obtained for each test. The average value of a_1 and η_1 , found from various tests are taken as the overall values of the hardening parameters a_1 and η_1 .

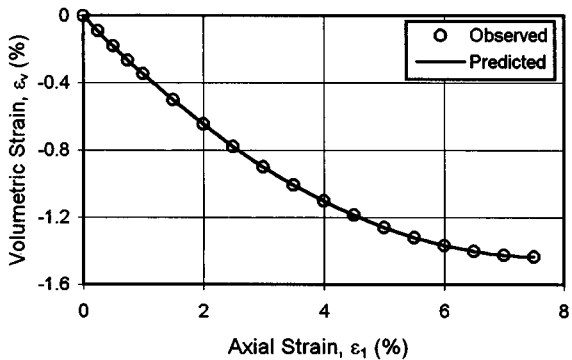
Nonassociative Parameter

The nonassociative parameter, κ [Eq. (7)] is determined based on the following equation:

$$\frac{d\varepsilon_v^p}{d\varepsilon_{11}^p} = \frac{\left(3 \frac{\partial Q}{\partial J_1}\right)}{\left(\frac{\partial Q}{\partial \sigma_{11}}\right)} \tag{29}$$

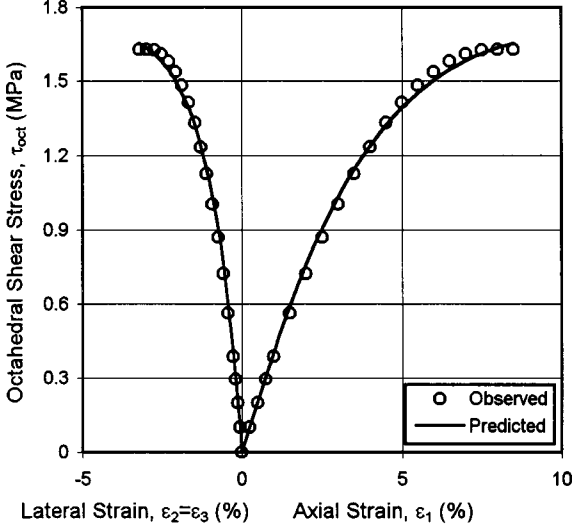


(a) Stress-Strain Behavior

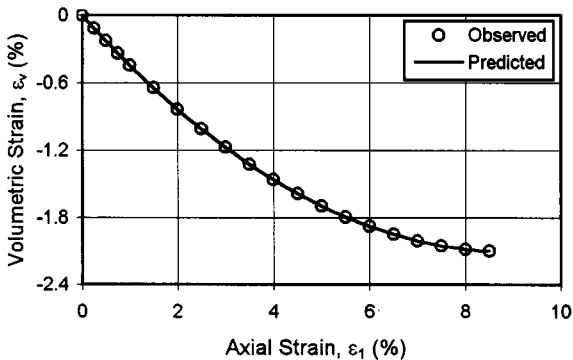


(b) Volume Change Response

Fig. 10. Stress-strain-volume change response of Ranjit Sagar rock-fill material ($\sigma_3 = 0.35$ MPa, $D_{\max} = 25$ mm) Group A prediction

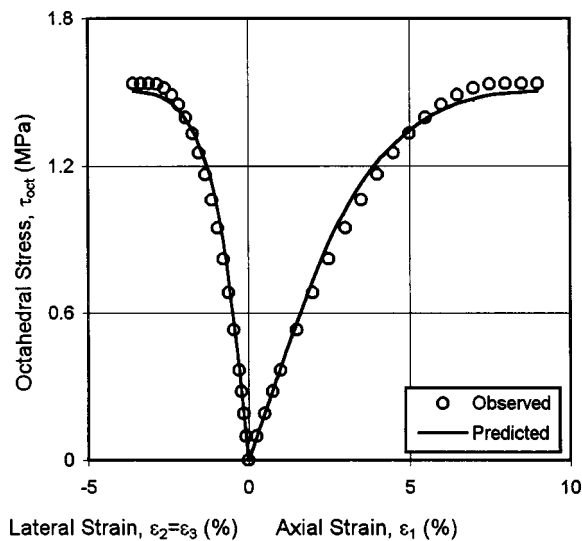


(a) Stress-Strain Behavior

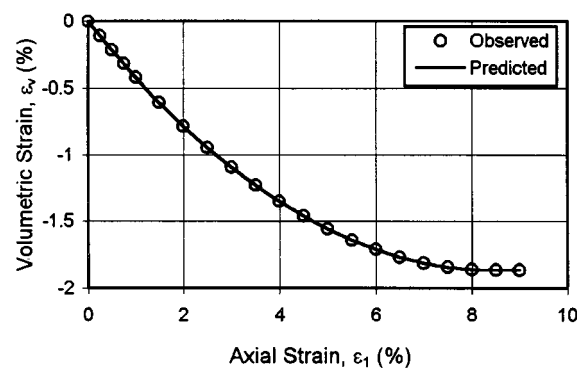


(b) Volume Change Response

Fig. 11. Stress-strain-volume change response of Ranjit Sagar rock-fill material ($\sigma_3 = 1.1$ MPa, $D_{\max} = 25$ mm) Group B prediction



(a) Stress-Strain Behavior



(b) Volume Change Response

Fig. 12. Stress-strain-volume change response of Ranjit Sagar rock-fill material ($\sigma_3 = 0.70$ MPa, $D_{\max} = 50$ mm) Group A prediction

where $d\epsilon_{11}^p$ = axial plastic strain increment; σ_{11} = axial stress; and $d\epsilon_v^p$ = volumetric plastic strain increment. The ratio of $d\epsilon_{11}^p/d\epsilon_v^p$ can be obtained from the slope of the observed $d\epsilon_{11}^p$ versus $d\epsilon_v^p$ response by choosing a point in the ultimate state. The value of α_Q which is represented on the right-hand side of Eq. (29) can then be found since the left-hand side is now known. Using this value along with α and r_v at the ultimate condition, the average value of κ is determined.

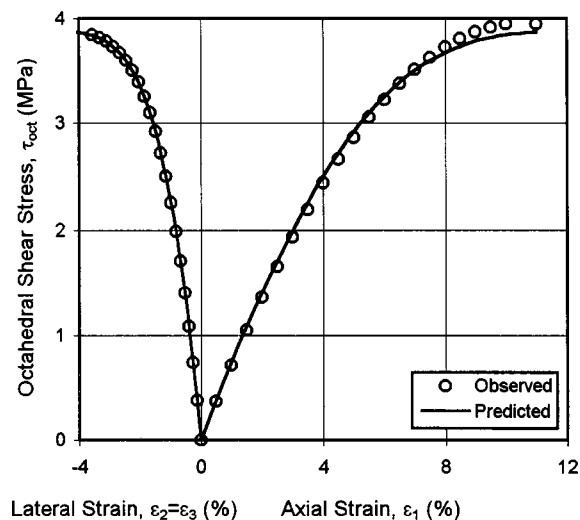
Elastic Parameters

The two elastic constants for an isotropic material, the Young's modulus E and Poisson's ratio μ are determined from the slope of the initial part of the stress-strain curve and the ratio of lateral strain to axial strain, respectively. The value of E is expressed as a function of confining pressure σ_3 using Janbu's (1963) relationship as

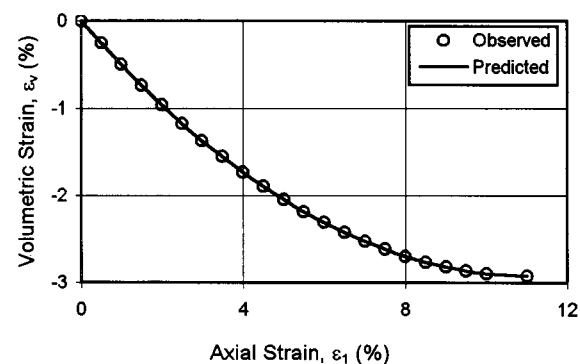
$$E_i = k P_a \left(\frac{\sigma_3}{P_a} \right)^{n'} \quad (30)$$

where k and n' are constants.

The material parameters were determined by using the following tests: for Ranjit Sagar rockfill, triaxial tests at confining pressures, 0.35, 0.70, and 1.40 MPa and for Purulia rockfill, triaxial tests at confining pressures, 0.3, 0.9, and 1.2 MPa. The material



(a) Stress-Strain Behavior



(b) Volume Change Response

Fig. 13. Stress-strain-volume change response of Ranjit Sagar rock-fill material ($\sigma_3 = 1.40$ MPa, $D_{\max} = 80$ mm) Group A prediction

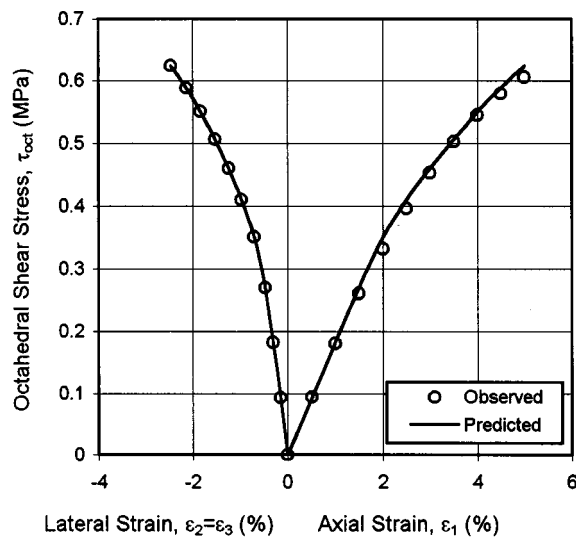
parameters obtained for the two rockfill materials are presented in Table 3. From the parameters, the following observations are made:

1. Elastic constant k increases with particle size for both materials, but the variation of n' shows an opposite trend. The value of μ decreases with particle size for both materials;
2. The values of the ultimate parameters, γ and β increase with particle size for Ranjit Sagar material, but the trend is opposite for the Purulia material;
3. The phase change parameter n is the same and is constant for both the materials;
4. The hardening parameter a_1 decreases and η_1 increases with the particle size for the Ranjit Sagar material, but the trend is reversed for the Purulia material; and
5. The disturbance parameters A and B increase with the particle size for Ranjit Sagar material, but the Purulia material shows the opposite trend.

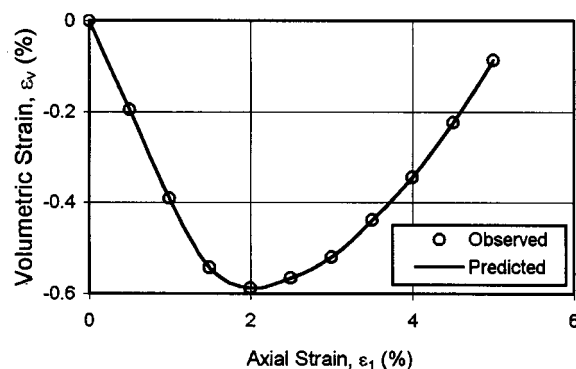
In general, the variation of material parameters with particle size is opposite for the two rockfill materials.

Predictions

The predictions of the stress-strain behavior of the two rockfill materials have been made by integrating the incremental stress-strain relationship



(a) Stress-Strain Behavior



(b) Volume Change Response

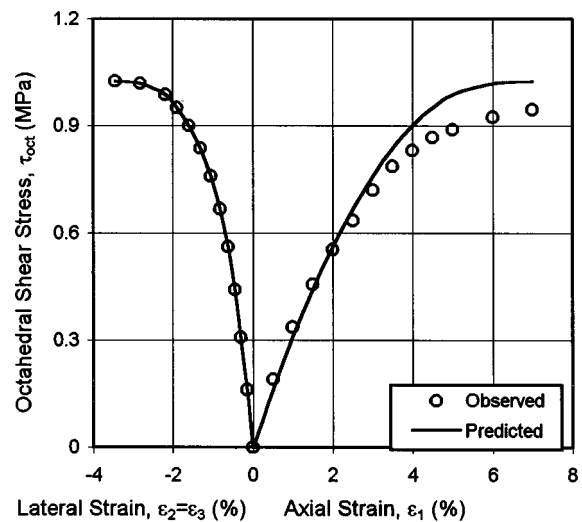
Fig. 14. Stress-strain-volume change response of Purulia rockfill material ($\sigma_3 = 0.30$ MPa, $D_{\max} = 25$ mm) Group A prediction

$$\{d\sigma\} = [C^{\text{DSC}}]\{d\varepsilon\} \quad (31)$$

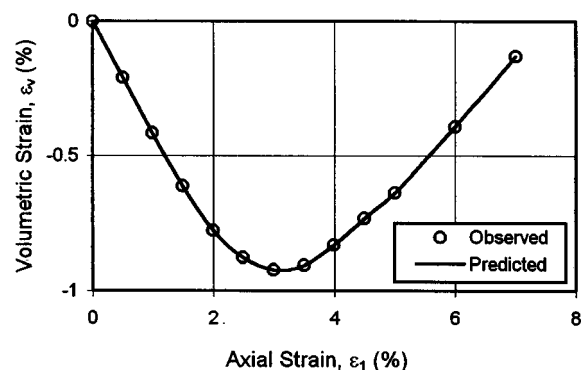
where $\{d\sigma\}$ and $\{d\varepsilon\}$ are the incremental stress and strain vectors and $[C^{\text{DSC}}]$ is the elastoplastic constitutive matrix derived based on the DSC (Gupta 2000).

Predictions have been made for two groups of tests, Group A—tests used for determining the material parameters and Group B—tests not used for evaluating the material parameters.

Each parameter is determined at different stages of the test. For example, γ and β are determined at the ultimate failure condition by setting $\alpha = 0$ in Eq. (4). The parameter κ is determined using the slope of the volume change curve close to failure. The parameters a_1 and η_1 are determined for each test using all data and average values are found for the material. It is to be noted that some parameters such as γ and β are determined using all the test results of a material and other parameters such as a_1 , η_1 , and κ are determined for each test and average of the values are taken for the material. Group A predictions are aimed at verifying whether, with the parameters obtained, the model is able to predict the stress-strain-volume change behavior of those tests used for determining the parameters. Group B predictions are meant to check the ability of the model to predict the stress-strain-volume change behavior of the tests not used for the determination of the material parameters. The predictions along with the observed results of a few tests are presented as detailed in Table 4.



(a) Stress-Strain Behavior



(b) Volume Change Response

Fig. 15. Stress-strain-volume change response of Purulia rockfill material ($\sigma_3 = 0.60$ MPa, $D_{\max} = 50$ mm) Group B prediction

Figs. 10–13 show the stress-strain-volume change behavior of Ranjit Sagar rockfill material. The predictions closely match the observed results for both Groups A and B tests. Figs. 14–17 show the stress-strain-volume change behavior of Purulia rockfill material. The predicted and observed results are very close to each other for both Groups A and B tests. As such, it may be concluded that the constitutive model provides satisfactory prediction of the stress-strain-volume change behavior of the two rockfill materials.

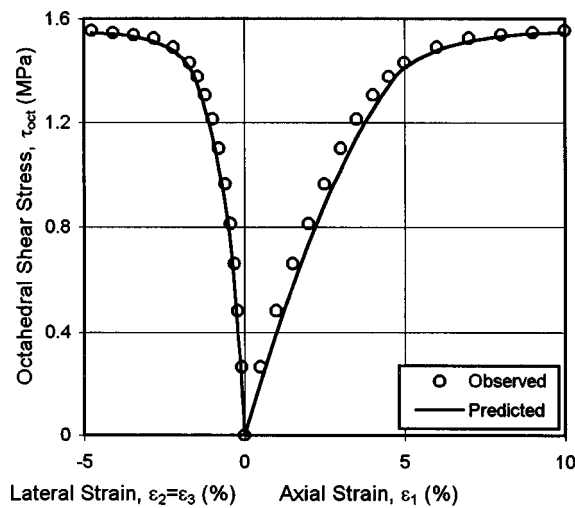
Material Parameters for Prototype Material

Material parameters for the prototype material were predicted using the material parameters for the various sizes of the modeled rockfill material. Based on the experience of predicting the material parameters for the rockfill materials using hyperbolic model (Venkatachalam 1993), an equation of similar form was used to predict the material parameters as follows.

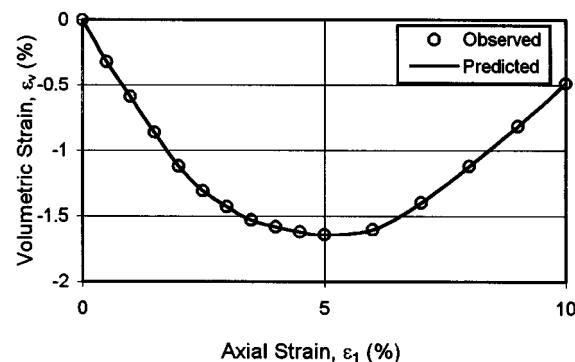
$$P = A_1 d_r^{A_2} \quad (32)$$

where P = parameter for the modeled rockfill material with the maximum particle size, D_{\max} and

$$d_r = \frac{D_{\max}}{D_{p \max}} \quad (33)$$



(a) Stress-Strain Behavior



(b) Volume Change Response

Fig. 16. Stress-strain-volume change response of Purulia rockfill material ($\sigma_3 = 1.2$ MPa, $D_{\max} = 80$ mm) Group A prediction

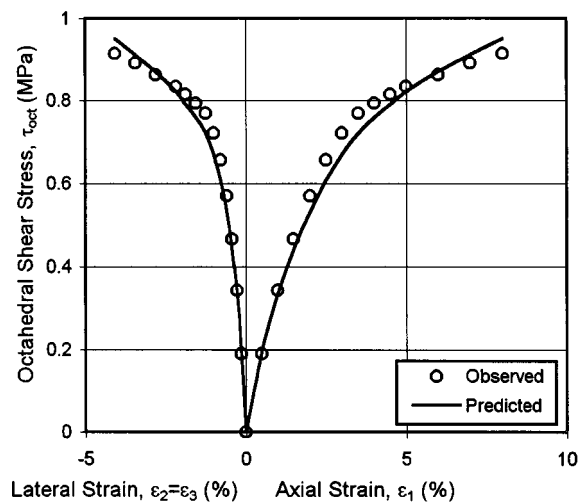
where $D_{p\max}$ = maximum size of reference rockfill material and A_1 and A_2 = constants.

Herein, the maximum prototype material size 320 mm for the Ranjit Sagar material and 1,200 mm for the Purulia material were used as the reference rockfill material.

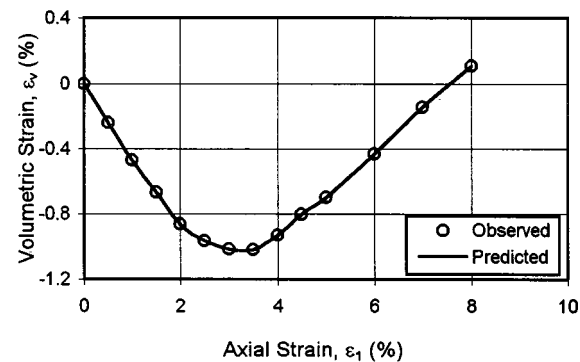
The constants A_1 and A_2 for various materials parameters were determined using the values of the parameters for the modeled rockfill materials given in Table 3. Regression analysis using the least-squares method was adopted for the curve fitting. The regression coefficients were found to be in the range of 0.95–1.00.

The parameters for prototype rockfill material were then computed by setting the value of d_r equal to unity. The values of the parameters, k , n' , γ , a_1 , η_1 , A , B , and ϕ determined are also given in Table 3. The effect of particle size on other parameters viz. μ , β , and κ was insignificant and therefore average values of these parameters are proposed as shown in Table 3. These material parameters for the constitutive model may be used for the analysis of the two rockfill dams.

It may be noted that the relationship given by Eq. (32) is empirical and the behavior of the prototype material as predicted from the material parameters obtained from the Eq. (32) herein cannot be verified directly by testing. However, the behavior can be verified indirectly by conducting an analysis of a rockfill dam using these material parameters and comparing the results with the field behavior by instrumentation.



(a) Stress-Strain Behavior



(b) Volume Change Response

Fig. 17. Stress-strain-volume change response of Purulia rockfill material ($\sigma_3 = 0.60$ MPa, $D_{\max} = 80$ mm) Group B prediction

Conclusions

Drained triaxial tests have been conducted on alluvial (rounded) and blasted (angular) rockfill materials obtained from two dam sites. Large size specimens were tested with high-confining pressures using large triaxial testing equipment. Stress-strain-volume change relationships of the materials were presented and discussed. The effect of size on the behavior of the two materials was found to be, in general, opposite for the two cases.

An elastoplastic model based on the disturbed state concept was used to depict the behavior of the two rockfill materials. This model is better than the available linear and nonlinear elastic models for rockfill materials as it allows for a number of factors such as irreversible plastic strains, plastic hardening, nonassociative (frictional) aspect, and degradation. The constitutive model is found to provide satisfactory prediction of the behavior of the two rockfill materials. Material parameters were predicted for the prototype rockfill material of large size and may be used for the analysis of the dam at the two project sites.

The procedure used for modeling the rockfill material, the triaxial tests conducted, the constitutive model used and the procedure used to predict the prototype material behavior appear promising and may be adopted for testing and modeling the behavior of the rockfill materials in general. However, field verification by instrumentation of the dam is essential to confirm the predictions

of the behavior of the dam made with the testing and constitutive modelling procedures adopted herein.

Acknowledgments

The research work was partly supported by Grant No. 16/INCGE-35/99 from the Ministry of Water Resources, Research and Development Division, Government of India. The assistance provided by the project authorities of the Ranjit Sagar and Purulia dams is gratefully acknowledged.

References

- Ansari, K. S., and Chandra, S. (1986). "How ought one to determine soil parameters to be used in the design of earth and rockfill dams." *Proc., Indian Geotechnical Conf.*, New Delhi, India, 2, 1–6.
- Desai, C. S. (1994). "Hierarchical single surface and the disturbed state constitutive models with emphasis on geotechnical applications." *Geotechnical engineering emerging trends in design and practice*, Chapter 5, K. R. Saxena, ed., Oxford and IBH New Delhi, India, Chap. 5.
- Desai, C. S. (1995). *Constitutive modeling using the disturbed state as microstructure self adjustment concept, continuum models for materials with microstructure*, H. B. Muhlhaus, ed., Wiley, Chichester, U.K., Chap. 8.
- Desai, C. S. (2001). *Mechanics of materials and interfaces: The disturbed state concept*, CRC Press, Boca Raton, Fla.
- Desai, C. S., Somasundaram, S., and Frantziskonis, G. (1986). "A hierarchical approach for constitutive modelling for geologic materials." *Int. J. Numer. Analyt. Meth. Geomech.*, 10(3).
- Desai, C. S., and Walthugala, G. W. (1987). "Hierarchical and unified models for solids and discontinuities (joints/interfaces)." *Implementation of constitutive laws for Engineering Materials*, C. S. Desai, ed., Short Course Notes, Univ. of Arizona, Tucson, Ariz.
- Frost, R. J. (1973). "Some testing experiences and characteristics of boulder-gravel fills in earth dams." *ASTM, STP*, 523, 207.
- Fumagalli, E. (1969). "Tests on cohesionless materials for rockfill dams." *J. SMFE, ASCE*, 95(SM1), 313–332.
- Gupta, A. K. (2000). "Constitutive modelling of rockfill materials." PhD thesis, Indian Institute of Technology, Delhi, India.
- Hall, E. B., and Gordon, B. B. (1963). "Triaxial testing using large scale high pressure equipment." *ASTM Symposium*, STP No. 361.
- Indian Standard Code IS: 2386. (1963). "Methods of test for aggregates for concrete. Part IV: Mechanical properties." Bureau of Indian Standards, New Delhi, India.
- Janbu, N. (1963). "Soil Compressibility as determined by oedometer and triaxial tests." *Proc., European Conf. Soil Mechanics and Foundation Engineering*, Wiesbaden, West Germany.
- Kachanov, L. M., (1958). *Theory of creep*, A. J. Kennedy, ed., National Lending Library, Boston (English translation).
- Kachanov, L. M. (1986). *Introduction to continuum damage mechanics*, Kluwer, Dordrecht, The Netherlands.
- Kulhawy, F. H., and Duncan, J. M. (1972). "Stresses and movements in Oroville dam." *J. SMFE*, 98(7), 653–665.
- Lambe, T. W., and Whitman, R. V. (1969). *Soil mechanics*, Wiley, New York.
- Lemaitre, J. A. (1984). "How to use damage mechanics." *Nucl. Eng. Des.*, 80, 237–245.
- Lemaitre, J. A. (1985). "Continuum damage mechanics model for ductile fracture." *J. Eng. Mater. Technol.*, 107, 83–89.
- Lowe, J. (1964). "Shear strength of coarse embankment dam materials." *Proc., 8th Int. Congress on Large Dams*, 3, 745–761.
- Marachi, N. D., Chan, C. K., and Seed, H. B. (1972). "Evaluation of properties of rockfill materials." *J. SMFE*, 98(1), 95–114.
- Marachi, N. D., Chan, C. K., Seed, H. B., and Duncan J. M. (1969). "Strength and deformation characteristics of rockfill materials." *Rep. No. TE 69-5*, Civil Engineering Dept., Univ. of California, Berkeley, Calif.
- Marsal, R. J. (1967). "Large scale testing of rockfill materials." *J. SMFE, ASCE*, 93(2), 27–43.
- Muhlhaus, H. B., and Vardoulakis, I. (1987). "The thickness of shear bands in granular materials." *Geotechnique*, 37, 271–283.
- Ramamurthy, T., and Gupta, K. K. (1986). "Response paper to how ought one to determine soil parameters to be used in the design of earth and rockfill dams." *Proc., Indian Geotechnical Conf.*, New Delhi, India, 2, 15–19.
- Saboya, F. J., and Byrne, P. M. (1993). "Parameters for stress and deformation analysis of rockfill dams." *Can. Geotech. J.*, 30(4), 690–701.
- Sudhindra, C., Venkatachalam, K., Soni, M. L., Sivakumar, N., and Sharma, P. (1991). "Large size triaxial shear tests on rockfill materials for design parameters." *Proc., 56th Research and Development Session*, CBIP, Hyderabad, 29–34.
- Theirs, G. R., and Donovan, T. D. (1981). "Field density gradation and triaxial testing of large-size rockfill for Little Blue Run Dam." *Laboratory shear strength of soil*, ASTM, STP 740, R. N. Yong and F. C. Townsend, eds., ASTM, 315–325.
- van Mier, J. G. M. (1991). "Mode-I fracture of concrete: Discontinuous crack growth and crack interface grain bridging." *J. Cement Concrete Res.*, 21, 1–15.
- Varadarajan, A., and Desai, C. S. (1993). "Material constants of a constitutive model: Determination and use." *Indian Geotech. J.*, 23(3), 291–313.
- Varadarajan, A., Sharma, K. G., and Soni, K. M. (1999). "Constitutive modelling of a reinforced soil using hierarchical model." *Int. J. Numer. Analyt. Meth. Geomech.*, 23, 217–241.
- Venkatachalam, K. (1993). "Prediction of mechanical behaviour of rock-fill materials." PhD thesis, Indian Institute of Technology, Delhi, India.
- Zeller, J., and Wullimann, R. (1957). "The shear strength of the shell materials for the Go-Schenenalp Dam, Switzerland." *Proc., 4th Inst. J on SMFE*, London, 2, 399–404.